

The effect of hydrostatic pressure on the activity and community composition of hydrocarbon-degrading bacteria in Arctic seawater

Angeliki Marietou,^{1,2} Jennie Spicker Schmidt,¹ Martin R. Rasmussen,¹ Alberto Scoma,^{1,2} Søren Rysgaard,³ Leendert Vergeynst^{2,3,4}

AUTHOR AFFILIATIONS See affiliation list on p. 14.

ABSTRACT There is a renewed interest in hydrocarbon biodegradation in Arctic seawaters due to increasing ship traffic and risk for oil spills. Most studies, however, fail to address the effect of increasing pressure as an environmental parameter. Here, we conducted a series of pressurized enrichments (0.1–30 MPa, 4°C) inoculated with a 100-day-old hydrocarbon-degrading biofilm collected from 615 m deep in Arctic seawater. Cell-specific CO₂ production rates provided a clear summary of the observed microbial activity: a bloom of a hydrocarbon degrading-biofilm generating 0.82–0.90 fmol CO₂·bacterial gene⁻¹·day⁻¹ at 0.1–8 MPa, but undetectable activity at 30 MPa until day 6. At 30 MPa, the microbial activity increased between days 6 and 34 with an average rate of 0.36 ± 0.08 fmol CO₂·bacterial gene⁻¹·day⁻¹. Amplicon sequencing revealed no differences in the microbial community composition at 0.1–12 MPa. While the typical Arctic alkane degraders *Oleispira* and *Shewanella* were abundant across all hydrostatic pressures and over time, *Colwellia*, *Neptunomonas*, and *Kiloniella* were significantly enriched solely at 30 MPa. Our results suggest that the physiological adaptations of psychophilic bacteria to thrive at sub-zero temperature make Arctic oil degraders tolerant to mild hydrostatic pressures of up to 12 MPa, whereas temperate climate communities have shown hydrostatic pressure-induced inhibition at 10–15 MPa in comparable studies. The activity of hydrocarbon degraders in sinking marine oil snow in the Arctic may remain unaffected down to depths of about 1,200 m, after which hydrostatic pressure can significantly affect hydrocarbon degradation at increasing depths down to 3,000 m.

IMPORTANCE Increased ship traffic in the Arctic region raises the risk of oil spills. With an average sea depth of 1,000 m, there is a growing concern over the potential release of oil sinking in the form of marine oil snow into deep Arctic waters. At increasing depth, the oil-degrading community is exposed to increasing hydrostatic pressure, which can reduce microbial activity. However, microbes thriving in polar regions may adapt to low temperature by modulation of membrane fluidity, which is also a well-known adaptation to high hydrostatic pressure. At mild hydrostatic pressures up to 8–12 MPa, we did not observe an altered microbial activity or community composition, whereas comparable studies using deep-sea or sub-Arctic microbial communities with *in situ* temperatures of 4–5°C showed pressure-induced effects at 10–15 MPa. Our results suggest that the psychophilic nature of the underwater microbial communities in the Arctic may be featured by specific traits that enhance their fitness at increasing hydrostatic pressure.

KEYWORDS Arctic, hydrocarbon biodegradation, psychophilic bacteria, hydrostatic pressure, microbial community

Editor Marina Lotti, University of Milano-Bicocca, Milano, Italy

Address correspondence to Leendert Vergeynst, leendert.vergeynst@bce.au.dk.

The authors declare no conflict of interest.

See the funding table on p. 15.

Received 19 June 2023

Accepted 5 October 2023

Published 9 November 2023

Copyright © 2023 American Society for Microbiology. All Rights Reserved.

Climate change is warming the Arctic faster than anywhere else on Earth reducing the extent of sea and land ice (1). As a result, it is expected that the Arctic seas will be open all year around for economic activities, such as shipping (2) and oil exploration (3), increasing the risk of unprecedented marine oil spills. Each year, about 3 million tons of oil enter the marine environment, 2.4 million tons of which is due to anthropogenic activities (4). We experienced the devastating oil spills, such as the Exxon Valdez spill in Alaska (1989), where 42 million liters of crude oil were spilled due to an oil tanker running aground, and the *Deepwater Horizon* spill in the Gulf of Mexico (2010), where 779 million liters of crude oil was spilled due to a rig explosion. Both incidents showed the long-term environmental effects and the technical limitations of recovering spilled oil from the Arctic and the deep seas (5, 6). Offshore oil drilling makes up to 37% of global oil production, with deep sea (>200 m depth) oil exploitation accounting for more than 12% (7). The US Geological Survey estimated that the Arctic seas and oceans contain 13% of the world's undiscovered oil reserves (3).

The average depth of the Arctic Ocean, Greenland Sea, and Baffin Bay is 1,040, 1,440, and 860 m, the deepest points being 5,500, 4,800, and 2,100 m below sea level (mbsl), respectively. This raises concerns for the anthropogenic release of oil hydrocarbons into the cold marine environment of the Arctic deep seas. Oil sinking to the deep sea depends on the oil's buoyancy, which is affected by various factors such as the oil's chemical composition, weathering, and the formation of aggregates with inorganic or biological particles. The density of sinking oil is primarily determined by the chemical composition, particularly oils such as bitumen and residual fuel oils with low content of aliphatic hydrocarbons and high content of asphaltenes may have a higher density than seawater. Weathering processes such as evaporation and biodegradation further reduce the content of low molecular weight aliphatic and aromatic hydrocarbons, thereby increasing the oil's density (8) and chances to eventually sink. Furthermore, oils tend to interact with mineral particles suspended in seawater, resulting in the formation of oil-mineral aggregates, a process that may occur when spilled oil mixes with sediment plumes originating at glaciers entraining mineral particles to tens of kilometers into the continental shelves (9). These aggregates may sink when the sediment-to-oil ratio in aggregates becomes too high (10).

Aggregates can also be formed with phytoplankton in combination with bacterial biofilms. Large marine oil-snow formations were observed in the oil-contaminated surface waters following the *Deepwater Horizon* oil spill (11). The formation of marine oil snow can impact the oil degradation process positively by increasing the exposed surface area of the oil and enhancing its biodegradation (12). However, marine oil snow has been observed to sink toward the seafloor, due to its increased density, thereby transporting the oil to the cold deep sea (13). This phenomenon represented the main cause for oil transfer to the seafloor at the *Deepwater Horizon* (14–16). The fate of microbial communities associated with oil-slick derived marine snow as it sinks down the water column is unclear. There is accumulating evidence suggesting that oil-slick derived marine snow can impact seafloor marine life by concentrating oil on the seafloor and attenuating oil degradation (17). At increasing depth, apart from low temperature, sinking biofilms are exposed to increasing hydrostatic pressure of 1 MPa for every 100 m increase in depth.

Despite a renewed interest on the effect of hydrostatic pressure on microbial activity since the *Deepwater Horizon* oil spill, there is a limited understanding of hydrocarbon degradation rates across the water column (18), particularly in the Arctic. Several studies have demonstrated that hydrocarbon degradation is affected even at moderate pressures of 10–15 MPa. Nguyen et al. (19) reported that the extent of *n*-alkane biodegradation was inversely proportional to hydrostatic pressure across a gradient of temperatures (4, 10, and 20°C). They estimated a 4% decrease in the rate of alkane degradation for every 1 MPa of pressure increase for communities sampled in the Gulf of Mexico at 1,000–1,500 mbsl with an *in situ* temperature of 4°C. Scoma et al. (20, 21) also reported that increasing pressure to 5–10 MPa negatively impacted

the hydrocarbon-degrading activity of two *Alcanivorax* species and observed an 8–9% reduced activity for every 1 MPa increase for a synthetic *n*-alkane degrading community adapted to 10 MPa. Marietou et al. (22) reported a 5% slower development per MPa at 15 MPa as compared to the growth and activity level observed at 0.1 MPa for communities sampled in the Gulf of Mexico at 1,100 mbsl with an *in situ* temperature of 4°C. Growth of an alkane-degrading *Rhodococcus* sp. isolated from surface seawater of the Norwegian Arctic was approximately twofold higher at atmospheric pressure (0.1 MPa) in comparison to 15 MPa (about 3.3% loss every 1 MPa increase) as reported by Schedler et al. (23). Prince et al. (24) used subarctic surface seawater from Newfoundland, Canada and examined oil biodegradation at 0.1 and 15 MPa, to discover that biodegradation was 33% slower at 15 MPa than at ambient pressure (about 2% loss every 1 MPa increase).

In this study, we examine the effect of hydrostatic pressure on a biofilm-derived hydrocarbon degrading community from an Arctic Fjord to assess the intrinsic capability of a psychrophilic autochthonous oil-degrading microbial community to degrade hydrocarbons at increasing hydrostatic pressure. In the Gulf of Mexico, surface water temperatures (up to 24°C) are substantially higher than the deeper waters (4°C), likely resulting in the seeding of deeper waters with mesophilic microbial communities. In contrast, at present studied location, the conditions are psychrophilic throughout the year and the water column has weak temperature gradients from the surface to deeper waters. This allowed us to conduct experiments in a context where the effect of pressure is isolated from the effect of temperature on the microbial community composition and activity over time.

MATERIALS AND METHODS

In situ incubations and sample collection

On May 29, 2018, moorings equipped with hydrophobic fluorocarbon-based adsorbents (Fluortex, Sefar Inc., production reference: 09-250/39) coated with marine gas oil were deployed in Godthåbsfjord, SW Greenland (64°37'00.5"N 50°56'55.6"W) at 615 mbsl at an *in situ* temperature of 1.4–1.8°C as described by Kampouris et al. (25) (Fig. 1). Marine gas oil (Kuwait Petroleum) is a diesel distillate from crude oil with low sulfur content (<0.05 mass%) and a low viscosity of <5 cSt at 40°C. At the same location, temperatures at the surface range from freezing during winter to 3°C during summer (26). The 3.2–16 µm thin oil film on the adsorbents provided a surface on which a native biofilm with hydrocarbon-degrading bacteria developed (25). Duplicate oil-coated adsorbents were collected after 8, 37, and 100 days and stored at –20°C for microbial community analysis following procedures described by Kampouris et al. (25). An additional two adsorbents collected after 100 days (6 September 2018) were stored in 50 mL Falcon tubes filled with native seawater and served as inoculum for the *ex situ* enrichments. The latter samples were stored for 36 days at 4°C until further processing (Fig. 1).

Ex situ pressurized enrichment microcosms

The stored adsorbents were washed with 5 mL artificial seawater and centrifuged to recover the microbial cells attached to the adsorbents. The autoclaved artificial seawater medium was saturated with pure oxygen and consisted of 32.5 g/L red sea salt in demineralized water, buffered with 25 mM 4-(2-hydroxyethyl)-1-piperazineethanesulfonic acid (HEPES) at pH 7.8 and amended with 50 µM NaNO₃ and 10 µM K₂HPO₄ as source of nitrogen and phosphorus. As pre-enrichment, six replicate 4.4 mL glass vials with artificial seawater medium, amended with 12.5 mg/L marine gas oil, were inoculated with 0.5 mL of the recovered biofilm suspension and sealed with a rubber cap without headspace. The vials were then placed in a 200 mL pressure vessel (Classic Filters Ltd., UK) and incubated at 4°C and 5.5 MPa for 14 days (Fig. 1).

Subsequently, for the final enrichments, the entire volume of the pre-enrichments (26.4 mL) was combined with 480 mL artificial seawater medium and saturated with pure oxygen (Fig. 1). Aliquots were subsequently transferred to 4.4 mL glass vials and

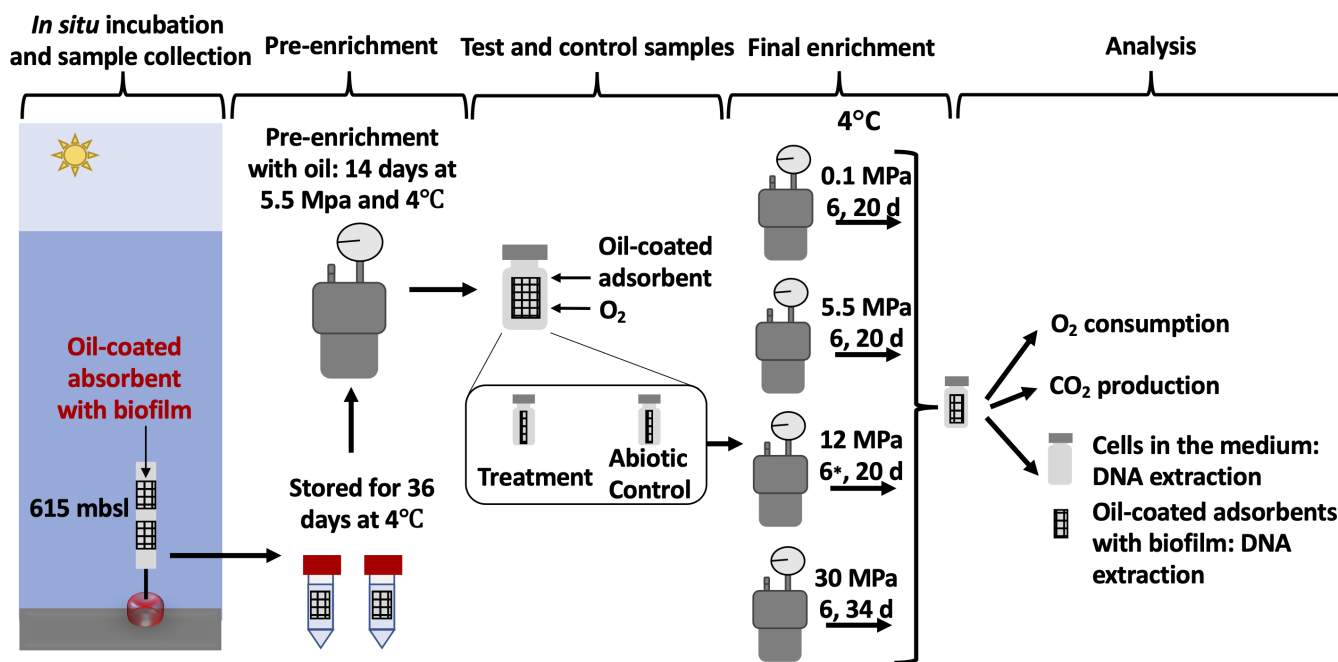


FIG 1 Schematic overview of the experimental design: Oil-degrading biofilms were collected in a Greenland fjord and used as inoculum for *ex situ* enrichment microcosms. After a pre-enrichment of 14 days at 5.5 MPa, test and control microcosms were inoculated and incubated at hydrostatic pressures between 0.1 and 30 MPa. The enrichment vials with 4.4 mL artificial seawater medium containing an oil-coated adsorbent of $40 \times 7 \text{ mm}^2$ were incubated inside the pressure vessels. Samples from the test and control microcosms were collected after 6–34 days for analysis of CO_2 production, 16S rRNA gene quantification by qPCR, and 16S rRNA gene amplicon sequencing. *The pressure in the pressure vessel at 12 MPa decreased to 8 MPa after 6 days.

sealed with a rubber cap. Fresh marine gas oil was supplied by adding a $40 \times 7 \text{ mm}^2$ oil-coated Fluortex adsorbent to each glass vial (Fig. 1). The adsorbents were prepared by dipping the adsorbent in marine gas oil, followed by 15 washes in demineralized water to remove superfluous oil resulting in approximately $2.8 (\pm 10\%) \text{ mg}$ marine gas oil per adsorbent. Abiotic controls were also prepared by adding $50 \text{ mg} \cdot \text{L}^{-1} \text{ HgCl}_2$ to inhibit biological activity. The enrichments were incubated at 4°C and over a range of hydrostatic pressures (0.1, 5.5, 12, and 30 MPa) corresponding to atmospheric pressure, 550, 1,200 and 3,000 mbsl, respectively (Fig. 1).

An oxygen microsensor was used to determine the residual oxygen concentration at the end of each incubation (27). To measure the overall mineralization of hydrocarbons, dissolved inorganic carbon was determined as described previously (28).

DNA extraction, quantification, and sequencing of bacterial 16S rRNA genes

At the end of the incubations, the oil-coated adsorbents with oil-associated biofilm were transferred to a 1.5-mL Eppendorf tube, while the cells in the medium were collected by centrifugation at 13,000 rpm for 5 min. Both the adsorbents and the cell pellet were stored at -80°C until further processing.

DNA was extracted using the method described by Lever et al. (29) with the following modification for optimized extraction efficiency as determined experimentally for our samples. A 0.5% Triton X-100 lysis solution was used that resulted in a 9–18% higher DNA yield. The DNA concentration was determined with the Quant-IT dsDNA High-sensitivity assay kit (Thermo Fisher Scientific) and a Qubit Fluorometer (Thermo Fisher Scientific).

The bacterial 16S rRNA gene copies were quantified using a SYBR green-based quantitative PCR (qPCR) as described previously (30) using the primers pair Bac908F/Bac1075R (31).

The community bacterial 16S rRNA genes were amplified and sequenced using the Illumina MiSeq platform with a paired-end 300 bp MiSeq v3 reagent kit following

procedures described by Vergeynst et al. (32) yielding 10,000–50,000 reads per sample. The 16S rRNA gene amplicon sequencing data from the enrichment experiments generated in this study are available at the NCBI Sequence Read Archive (SRA) under BioProject accession number [PRJNA944198](#). The data from the field is a subset of previously published data (accession number [PRJNA884198](#)) by Kampouris et al. (25).

Data analysis

The sequence reads were processed using DADA2 version 1.16.0 (33) in R version 4.0.5 as described previously (34) resulting in 2,131 amplicon sequence variants (ASVs). A total of 982 bacterial ASVs were retained representing 98.3% of all reads after excluding chloroplast ASVs and ASVs that occurred in only one sample. ANOVA-like differential expression analysis (ALDEx2) using the logit transform was applied to identify differentially abundant taxa between treatments (35). Benjamini-Hochberg corrected *P* values were used to control the overall false discovery rate to 5%. Principal component analysis (PCA) and redundancy analysis (RDA) were performed using the R-package “Vegan” (36) on logit-transformed relative abundances (37). A geometric Bayesian-multiplicative treatment was applied to replace zero counts with expected values using R-package “zCompositions” (38). Variance partitioning based on partial RDA was performed to estimate the variance of the community compositions explained by the experimental treatments (39).

For selected ASVs, closely related sequences from cultured and/or environmental samples were identified and retrieved using NCBI’s Blast webservice with the blastn option (40). Selected ASVs (those significantly different in abundance at higher pressure) and closely related sequences were used for constructing maximum likelihood phylogenetic trees in RAxML (41) using the GTR substitution model. The phylogenetic trees were visualized using iTOL (42).

In the pressurized experiments, CO₂ production was used as a measure of microbial activity. Due to limitations of cell counting in biofilms, 16S rRNA gene counts measured by qPCR were used as a proxy for cell counts. The average 16S rRNA gene-specific CO₂ production rate ($q = \frac{C_t - C_0}{\bar{X}t}, \frac{\text{mol CO}_2}{\text{gene copy} \cdot \text{day}}$) was estimated as the ratio of the CO₂ production rate in the enrichment vials ($\frac{C_t - C_0}{t}$) to the average suspended and biofilm-associated 16S rRNA gene concentration measured by qPCR (\bar{X}).

The concentration of gene copies associated with the biofilm (gene copies cm⁻²) was estimated from the total qPCR count of gene copies in biofilm extracts normalized to the surface area of the adsorbents (adsorbents of 40 × 7 mm² with biofilm on both sides giving 5.6 cm²) on which the biofilms developed (32). The fraction of 16S rRNA gene copies in the biofilm ($\frac{\text{gene copies in biofilm}}{\text{gene copies in biofilm} + \text{gene copies in medium}}$) was calculated from the total count of gene copies detected in the medium and in the biofilms on the adsorbents.

RESULTS

Growth and CO₂ production patterns

A series of enrichments were set up using as inoculum a 100-day-old hydrocarbon-degrading biofilm from a field experiment at 615 mbsl in Arctic seawater (25). In the enrichments, oil-degrading bacteria grew as biofilms on oil-coated adsorbent and were suspended in their surrounding medium. The incubation period (end point) was decided based on the oxygen depletion patterns for each set of enrichments. As such, incubations were terminated after 6 and 20 days at all pressures except for the 30 MPa incubations, which were terminated after 6 and 34 days. We did not observe oxygen consumption (Table S1) or CO₂ production in the abiotic controls confirming that any observed change in the inoculated tests was due to microbial activity (Fig. 2A). At

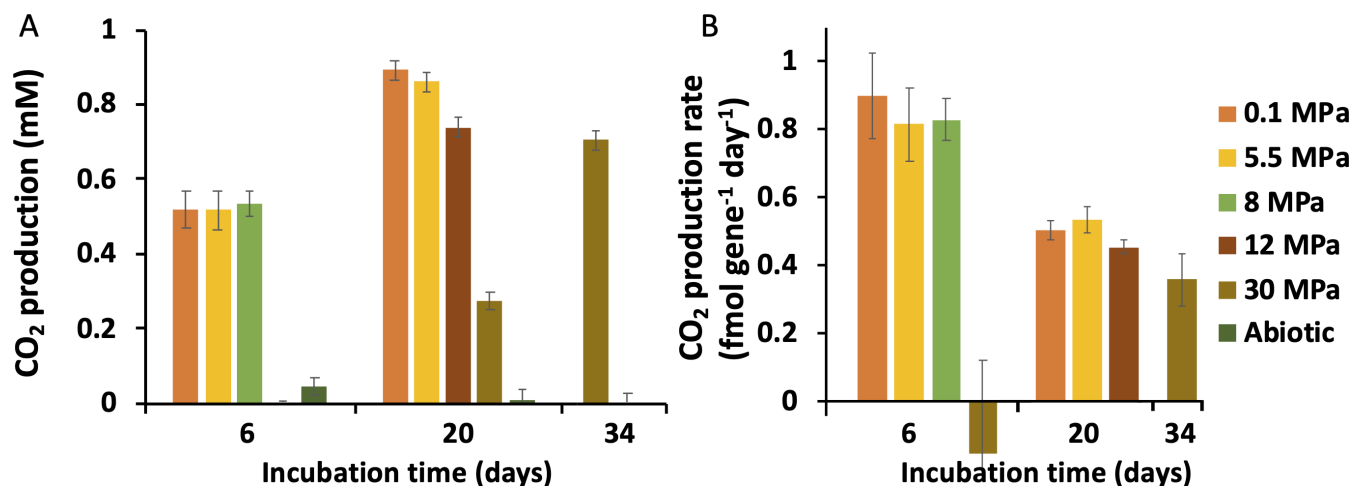


FIG 2 CO₂ production (A) and average 16S rRNA gene-specific CO₂ production rate (B) in the enrichments after 6, 20, and 34 days of incubation at hydrostatic pressure of 0.1, 5.5, 8, 12, and 30 MPa ($n = 3$). The average 16S rRNA gene-specific CO₂ production rate was estimated using the ratio of the CO₂ production rate in the enrichment vials to the average suspended and biofilm-associated 16S rRNA gene concentration measured by qPCR.

pressures of 0.1, 5.5, and 8 MPa, we observed a decrease in oxygen (from 100% to 27–44% saturation, Table S1) and about 0.52–0.53 mM increase in CO₂ concentration as early as day 6, indicating significant microbial activity (Fig. 2A). Over the course of the experiment, one of the pressure reactors used for the 12 MPa incubations lost hydrostatic pressure and had a registered pressure of 8 MPa at day 6. Hence, we have recorded one time point at 8 instead of 12 MPa as it is not known when the decompression took place over the 6-day incubation period. The CO₂ production of the 0.1, 5.5, and 12 MPa incubations further increased to 0.86, 0.89 and 0.74 ± 0.03 mM, respectively, at day 20 (Fig. 2A), when oxygen was completely depleted (<0.5% saturation) and the bacteria were limited in oxygen as final electron acceptor. A substantial reduction in microbial activity due to hydrostatic pressure was seen at 30 MPa, where CO₂ production was about 11 times lower at day 6 and oxygen was still available during the whole incubation period (67 and 15 ± 3% saturation after 20 and 34 days, respectively). At day 34, a CO₂ production of 0.70 mM was reached, approaching the values observed for the lower pressure microcosms (0.74–0.89 mM) at 20 days.

The observed CO₂ production can be explained by the degradation of hydrocarbons because marine gas oil, which is a mixture of hydrocarbons with a typical elemental composition of 86–88%C, 11–13%H, <0.1%N, <0.1% S, and <2.5%O (43, 44), was the only carbon source provided. From the latter and the 0.70–0.89 mM CO₂ production at the end of the incubations, it can be estimated that 1.5–1.9% of carbon from the 2.8 mg marine gas oil initially coated on the adsorbents was completely mineralised to CO₂. The accumulated CO₂ could also be produced from decaying cells. However, the cell content of the inoculum could only contribute to about 0.001–0.1 mM CO₂ production, which is 0.1–11% of the highest observed CO₂ production of 0.9 mM after 20 days at 0.1 MPa. The latter was estimated from the initial 8.3·10⁶ 16S rRNA gene copies·mL⁻¹ and assuming 1–5 16S rRNA gene copy per cell and a cellular C content of 10–149 fg·cell⁻¹ (45–47). These estimates confirm that the observed CO₂ production is an appropriate measure for the activity of hydrocarbon degraders.

The observed differences in oxygen consumption and CO₂ production over time reflected the estimated bacterial cell growth, as determined by the number of bacterial 16S rRNA gene copies in the medium and biofilm of the enrichments (Fig. 3). The initial bloom of bacterial cells was clearly driven by biofilm formation as at day 6 the majority (91–93%) of the 16S rRNA gene copies were associated with the biofilm for the lower hydrostatic pressures (0.1, 5.5, and 8 MPa) microcosms. In the medium though, we observed a slow initial 1.6- to 1.8-fold increase in copy number until day 6. Between

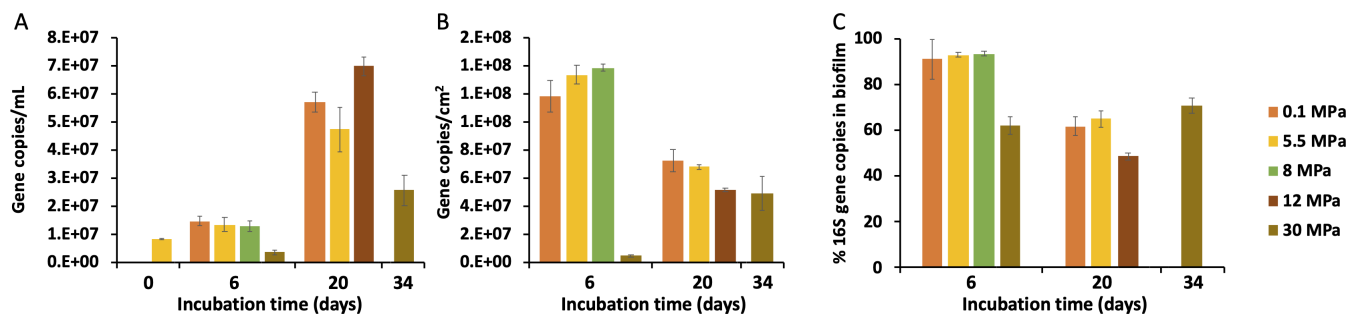


FIG 3 16S rRNA gene copy numbers in the enrichments over time in (A) the medium of the enrichments and (B) extracted from the biofilms on the oil-coated adsorbents in the enrichments. (C) The fraction of 16S rRNA gene copy numbers associated with the biofilms on the oil-coated adsorbents relative to the total copy number measured in the biofilms and the surrounding medium of the enrichments ($n = 3$). At the different time points (0, 6, 20, and 34 days), bacterial DNA was extracted directly from the oil-coated adsorbents with oil-associated biofilm (A), while the cells in the medium (B) were collected by centrifugation before DNA extraction.

days 6 and 20, biofilm copy numbers decreased by 40–50%, coinciding with a 5.7- to 8.4-fold increase in the medium. These results indicate that the biofilm community that developed during the first 6 days likely seeded the community in the medium (free-living fraction) between days 6 and 20. Growth kinetics at 30 MPa were different as compared to lower hydrostatic pressures: there was a substantially slower growth until day 6 as evidenced by biofilm copy numbers of about 30-fold lower than at 0.1–8 MPa, and decreasing copy numbers in the medium (free-living). Between days 6 and 34, the gene copy numbers increased both in the medium and the biofilm, with slightly higher numbers in the biofilm fraction (62–71%). The measured copy numbers at day 34 at 30 MPa were in the same order as at day 20 with the lower hydrostatic pressures.

Combining CO_2 production with copy numbers to estimate cell-specific CO_2 production rates provided a clear summary that was consistent with the previously discussed patterns (Fig. 2B): an initial biofilm-dominated bloom of oil degraders with high microbial activities of $0.82\text{--}0.90 \text{ fmol CO}_2 \cdot \text{gene}^{-1} \cdot \text{day}^{-1}$ at 0.1–8 MPa, but undetectable activity at 30 MPa until day 6. After day 6, the lack of oxygen likely caused the average rates to drop to $0.50\text{--}0.53 \text{ fmol CO}_2 \cdot \text{gene}^{-1} \cdot \text{day}^{-1}$ at 0.1 and 5.5 MPa and $0.45 \pm 0.02 \text{ fmol CO}_2 \cdot \text{gene}^{-1} \cdot \text{day}^{-1}$ at 12 MPa until day 20, whereas at 30 MPa microbial activity increased to an average rate of $0.36 \pm 0.08 \text{ fmol CO}_2 \cdot \text{gene}^{-1} \cdot \text{day}^{-1}$ until day 34.

Characterization of the microbial community

The *in situ* hydrocarbon-degrading microbial communities in the biofilm collected at 615 mbsl in the Arctic were characterized by an initial fast increase of Gammaproteobacteria driven by *Oleispira* sp. ($93 \pm 1\%$ at day 8, Fig. 4A). From day 37 until day 100, the dominance of *Oleispira* sp. decreased, which was associated with the depletion of aliphatic hydrocarbons (25). Simultaneously, a more diverse community arose including the genera *Arcobacter* ($16 \pm 6\%$ at day 37), *Colwellia* ($20 \pm 7\%$ at day 37), *Pseudofulvibacter* ($10 \pm 3\%$ at day 37), and *Cycloclasticus* ($9 \pm 8\%$ at day 100) associated with the degradation of polycyclic aromatic hydrocarbons (25).

For the *ex situ* pressurized incubations, 16S rRNA amplicon sequencing of the medium and biofilm-associated communities revealed that, despite temporal and pressure-related changes (Fig. 2 and 3), the community was at all times and pressures dominated by two gammaproteobacterial: *Oleispira* sp. [ASVs with 100% and 98% identity score to *Oleispira antarctica* RB-8 (ASV6)]; and *Oleispira lenta* DFH11 (ASV241) (Fig. 4B; Fig. S1 and S2). Another gammaproteobacterial ASV abundant across the different pressures and over time belonged to *Shewanella arctica* IR12 (100% identity score) (ASV736, Fig. 4B). Despite the presence (16%) of *Cycloclasticus* sp. (ASV28; 100% identity score) in the pre-enrichment, its relative abundance decreased in all enrichments (Fig. 4B). Gammaproteobacteria dominated (about 90% relative abundance) both the medium

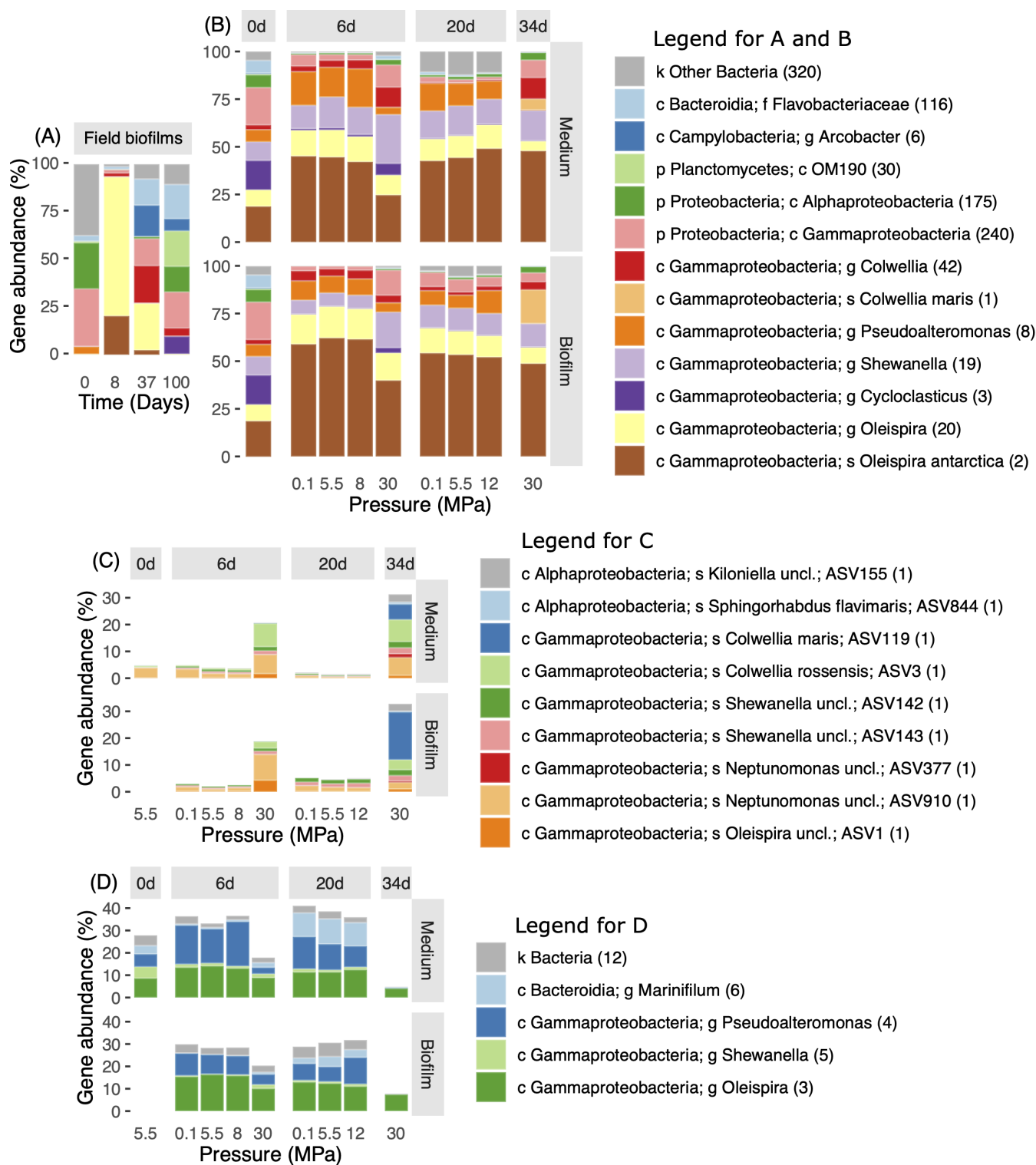


FIG 4 Mean ($n = 3$) relative abundances of bacterial 16S rRNA genes as a function of time and hydrostatic pressure in field biofilms (A) and in the medium and biofilm of laboratory enrichments (B), and taxa that had a significantly higher (C) and lower (D) relative abundance at 30 MPa as compared to the lower pressures. The plots were constructed as follows: first, taxa classified down to the species level having a relative abundance higher than a cutoff value in at least one of the treatments were plotted. The cutoff was 13%, 13%, 0%, and 5% for subplots (A), (B), (C), and (D), respectively. The same procedure was subsequently repeated at the taxonomic levels of genus, family, order, class, and phylum using the same cutoff value. Finally, relative abundances of the remaining taxa for which the relative abundance at the phylum level was lower than the cutoff value were summed up and denoted “other bacteria.” The number of ASVs for each taxon is indicated between brackets.

and the biofilm-associated microbial community of the enrichments across the different pressures and over time (Fig. 4B).

The enrichment communities were clearly influenced by the *in situ* oil-associated biofilm community, as 22 ASVs with a relative abundance of at least 1% in the enrichments were also detected in the field biofilms. Taken together, these 22 ASVs represented about 50–75% of the total community of the enrichments, but only 3–20% in the field biofilms. Only two ASVs (*O. antarctica*, ASV6, and *Cycloclasticus* sp., ASV28) were observed at abundances of more than 5% in both the field and enrichment communities. Hence, species present only at low levels in the field eventually dominated the lab enrichments. These differences in composition may be attributed to the specific incubation conditions in the enrichments such as temperature, nutrient amendment and higher concentration of dissolved hydrocarbons.

The pressure-induced changes of the alpha- and beta-diversity of the microbial community over time were analyzed based on the Shannon diversity index and by PCA and RDA analysis, respectively. The Shannon diversity (Fig. S3) decreased over time for all treatments and was generally lower for communities in the biofilm than in the medium which can be associated with the greater dominance of in particular the genus *Oleispira* in the biofilm communities (Fig. 4B). The decrease in diversity was slower at 30 MPa than at the lower pressures, which reflected the lag phase in microbial activity (Fig. 2) and the associated slower community succession at 30 MPa (Fig. 4B). The microcosm composition of the communities diverged as a function of time, with the 0.1, 5.5, 8, and 12 MPa samples (biofilm and free-living) clustering separately from the 30 MPa samples already at day 6, and diverged completely by days 20 and 34 (Fig. 5A). When considering all samples, ANOVA and variance partitioning based on RDA showed that pressure, as well as the other parameters, such as time, CO₂ production, and the matrix (biofilm or medium), had significant marginal effects ($P < 0.05$) on the community compositions. These variables explained (adjusted R^2) individually 9%, 14%, 20%, and 6%, respectively, and together 47% of the total variance (Fig. 5). ALDEx2-based ANOVA confirmed the pressure-induced differences in community composition and allowed to identify the ASVs that were affected by pressure. When comparing the ASV's abundances between the lower pressures (0.1, 5.5, and 12 MPa) at 20 days, none of the ASVs showed to be differentially abundant. However, the abundance of 30 and 9 ASVs were significantly ($P < 0.05$) lower and higher, respectively, at 30 MPa after 34 days as compared to the lower pressures (0.1–12 MPa) after 20 days. The genera that were significantly negatively affected at 30 MPa as compared to lower hydrostatic pressures were *Pseudoalteromonas*

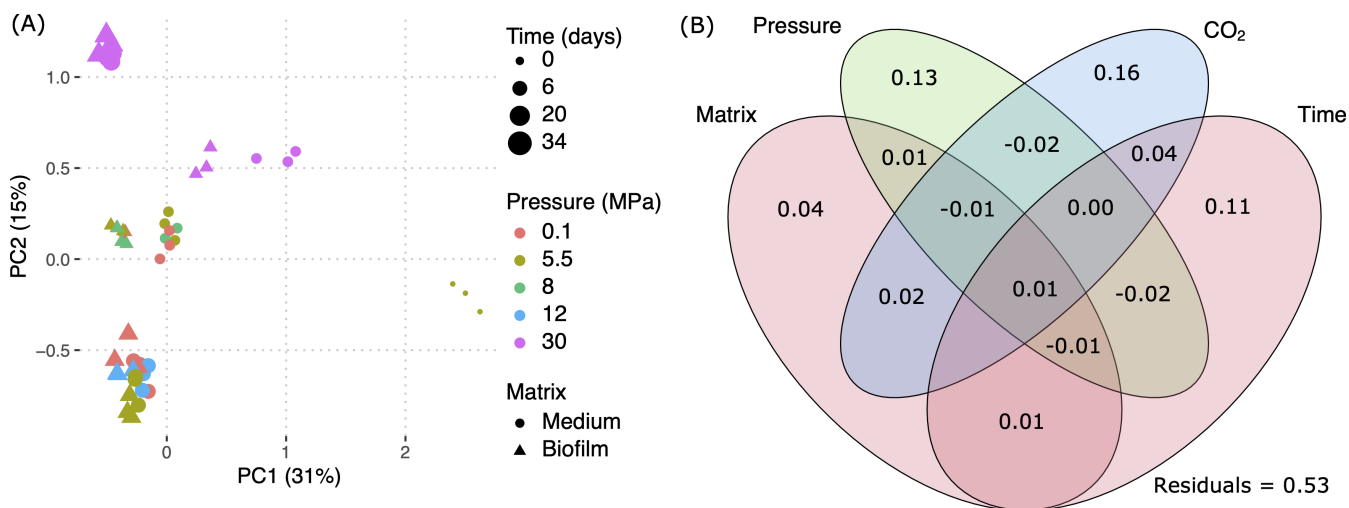


FIG 5 Score plot of the PCA (A) and variance partitioning of the RDA (B) on the microbial community composition determined by 16S rRNA gene sequencing in the enrichments at 0, 6, 20, and 34 days and hydrostatic pressures of 0.1, 5.5, 8, 12, and 30 MPa. The factor matrix with levels *Biofilm* and *Medium* refers to the DNA extracted from the biofilms on the oil-coated adsorbents and the cells collected from the medium of the enrichments, respectively.

sp. (four ASVs) and *Mariniflum* (six ASVs), contributing to 7–14% and 2–11%, respectively, of the community after 20 days in the 0.1–12 MPa enrichments, but less than 0.3% at 30 MPa (Fig. 4D and 6). The nine 30 MPa-associated ASVs represented 19–33% and 2–5% of the communities (at 30 MPa and 0.1–12 MPa, respectively), showing that a substantial fraction of the community at 30 MPa could be clearly associated with piezophilic conditions (Fig. 4C). Among those ASVs, four ASVs classified as the Gammaproteobacteria *Colwellia maris* ABE-1 (ASV119, 100% sequence identity), *Colwellia rossensis* S51-W (ASV3, 99% identity), *Neptunomonas antarctica* S3-22 (ASV910, 99% identity), and the Alphaproteobacterium *Kiloniella antarctica* soj2014 (ASV155, 99% identity) showed to be strongly associated with incubations at 30 MPa and contributed to 6–18%, 4–8%, 2–7%, and 3% of the community at 34 days (Fig. 4C and 6).

Figure 7 shows the phylogenetic relationships among the ASVs with significantly ($P < 0.05$) higher relative abundance at 30 MPa, closely related isolates, and selected piezophiles. The majority of the ASVs were closely related to sequences recovered from low-temperature environments such as the Antarctic Sea (48, 49), Norwegian deepwater coral reefs (50), Antarctic sponges from the Terra Nova Bay (Ross Sea) (51), subarctic glacial Fjord (Kongsfjorden) (52), and deepwater subarctic sediments (Faroe-Shetland Channel) (53). Most psychropiezophilic strains isolated to date, belong to gammaproteobacterial lineages such as *Colwellia* and *Shewanella* (54), to which *C. maris* (ASV119), *C. rossensis* (ASV3), and *S. arctica* IR12 (ASV736) were close relatives (Fig. 7).

DISCUSSION

Our study offers a novel insight into the effect of hydrostatic pressure isolated from the effect of temperature on microbial hydrocarbon degradation in the Arctic. This was achieved by utilizing *in situ* grown hydrocarbon-degrading biofilms under psychrophilic condition in a water column with weak temperature gradients from the surface to deeper waters. The Arctic biofilm-derived, oil-degrading community used as inoculum in the *ex situ* pressurized microcosm experiments was naturally adapted to life at psychrophilic conditions (1.4–1.8°C) and hydrostatic pressures of about 6 MPa. Its microbial community assemblage was similar to previous communities from our *in situ* studies in the same Arctic fjord system, with the enriched autochthonous bacteria possessing oil-degrading capacity even at near- or sub-zero temperatures (32, 34, 55). The initial *Oleispira*-dominated bloom is typical for an aliphatic hydrocarbon biodegrading community, as observed in our previous Arctic field studies at a nearby sampling location (32, 34). Several genera of the more diverse community observed from day 37 until day 100 have been associated with degradation of monocyclic and polycyclic aromatic hydrocarbons (56). Samples from our previous Arctic studies indicated that *n*-alkanes can be degraded with a half-life time of 20–36 days, followed by branched- and cycloalkanes with a half-life of 56–111 days, and 3- and 4-ring polycyclic aromatic compounds with a half-life of 120–252 days (25). The observed overall mineralization of 1.5–1.9% over the duration of our *ex situ* incubation of 20–34 days is in the range of the mineralization of 2.8% over 20 days observed in previous lab incubations at the same temperature of 4°C (28). A limitation of the present study is the lack of data regarding the degradation of specific hydrocarbons. However, in our previous lab study (28), we observed that all *n*-alkanes and naphthalene were degraded at rates of about 10 times higher than the rate of mineralization, low-molecular weight polycyclic aromatic compounds (C_{1-3} -naphthalenes, C_{0-1} -phenanthenes, and C_{0-1} -fluorenes) at about 5–10 times higher rates than the mineralization and the other polycyclic aromatic compounds with more rings and alkylation at rates similar to the overall mineralization. Hence, taking into account our previous lab (28) and field (25) studies, it may be expected that the degradation of in particular *n*-alkanes and some low-molecular-weight polycyclic aromatic compounds contributed to the observed CO₂ production. It is unlikely that hydrocarbons with a more complex chemical structure and lower degradation rates such as branched- and cycloalkanes and high-molecular-weight polycyclic aromatic compounds that are typically degraded over time scales of months contributed

substantially to the observed CO₂ production. The results of this study represent thus the initial degradation of the most biodegradable fraction of the oil. In the present investigation, the averaged CO₂ production kinetics (Fig. 1), microbial community growth dynamics (Fig. 2C) and estimated cell number (based on 16S rRNA gene copies on biofilms or as freely suspended cells, Fig. 2A and B) indicate that the oil-degrading process between 0.1 and 12 MPa (surface to 1,200 mbsl) was essentially similar. On the contrary, a hydrostatic pressure of 30 MPa (3,000 mbsl) negatively impacted the growth and activity of the enriched hydrocarbon degraders (Fig. 2 and 3).

Considering that we used an autochthonous psychrophilic community that was adapted to the *in situ* temperature of 1.4–1.8°C and subsequently incubated at 4°C, we can isolate the effect of pressure, knowing that any changes in the community structure and activity are mainly due to the effect of the pressure treatment alone. Microbes thriving in polar regions have a series of mechanism allowing them to be physiologically adapted to low temperatures such as (i) synthesis of unsaturated fatty acids to maintain membrane fluidity, (ii) cold shock proteins that act as molecular chaperons assisting transcription and translation, (iii) increase resistance by “switching” to viable but non-culturable cells capable of performing essential functions but not growing or dividing, (iv) production of antifreeze proteins that bind to ice crystals to prevent their growth and recrystallization, (v) and production of psychrophilic enzymes (57). Modulation of membrane fluidity and composition is the most well-studied high-pressure adaptation (58), with deep-sea organisms ranging from fish to bacteria able to increase the level of unsaturated fatty acids in response to increasing pressure. Grossi et al. (59) reported higher unsaturated fraction in the membrane and storage lipid composition at 35 MPa for the piezotolerant alkane-degrading *Marinobacter hydrocarbonoclasticus*. Studies in the deep-sea bacterium *Photobacterium profundum* SS9 (60) and the mesophile *Escherichia coli* (61) have demonstrated that the production of unsaturated fatty acids alone does not confer adaptation to high pressure (piezoadaptation), but it can be of an advantage and quite possibly increase the pressure-tolerance and enable the unsaturated fatty acid isolates to remain active over a wider range of pressures. For this reason, it has been suggested that there may be some overlap between psychrophilic and piezophilic adaptations (62, 63). This is for instance reflected in the fact that: (i) isolated piezopsychrophiles typically have the lowest optimal hydrostatic pressures (as low as 10 MPa) within all isolated piezophiles so far; and (ii) all isolated (hyper)piezopsychrophiles generally require lower hydrostatic pressures to grow optimally as compared to their capture depth. The similarity between the adaptation strategies to cold temperatures and increased hydrostatic pressures possibly entail that piezopsychrophiles may even be isolated from permanently cold surface waters from polar regions (as the Arctic) (64). In other words, microbial seeding from permanently cold surface waters provides deeper water layers with communities that are less inhibited by increasing hydrostatic pressures as compared to lower, warmer latitudes.

Our results showed that mild hydrostatic pressures of up to 8–12 MPa did not substantially impact the hydrocarbon degradation rates of an Arctic community exposed to year-round psychrophilic conditions throughout the water column. We did not observe an altered community composition and the cell-specific activity was reduced by about 1% every 1 MPa increase over the range of 0.1–12 MPa. This hydrostatic-pressure-induced effect is substantially lower than in comparable studies discussed in the introduction: deep sea communities from temperate climates showed pressure-induced effects at 10–15 MPa with 4–9% reduced activity per MPa increase (19–22) and an Arctic isolate and a community from a subarctic environment transferred to 15 MPa showed 2–3% reduced activity per MPa increase (23, 24). On the contrary, reactors subjected to 30 MPa showed an altered community composition and lower cell-specific activity as compared to reactors incubated at ≤12 MPa. This aligns with the proposed 10–20 MPa as the transition hydrostatic pressure range above which a competitive advantage is set for microorganisms that are specifically adapted to piezophily (64).

The enrichments irrespective of the pressure conditions consisted mainly of gammaproteobacterial hydrocarbon degraders, dominated by the genera *Oleispira* and *Shewanella* (Fig. 4B). These genera are known alkane degraders and we have associated them in previous *in situ* Arctic studies with an early stage biofilm degrading mainly alkanes (32). Despite the use of a mature biofilm of 100 days old, the addition of fresh oil triggered the proliferation of fast-growing first responders, while degraders of complex polycyclic aromatic hydrocarbons such as *Cycloclasticus* sp. (ASV28) that are typical for mature oil-degrading biofilms (25) were out-competed. Similarly, the *in situ* Gulf of Mexico oil plume samples with an average temperature of 5°C were dominated by psychrophilic and psychrotolerant gammaproteobacterial species, while more than 90% of all sequences belonged to a single Oceanospirillales ASV (65). *O. antarctica* RB-8 was originally isolated from an enrichment culture of surficial seawater samples in Rod Bay (Ross Sea, Antarctica); it is able to degrade alkanes using an array of alkane monooxygenases, and produces osmoprotectants that could facilitate cold adaptation (48, 66). The prevailing *O. antarctica* RB-8 (ASV6) together with *O. lenta* strain DFH11 (ASV241) are reported to be able to modulate their cellular fatty acid profile in response to temperature changes (low temperature), an ability that is also connected with adaptation to pressure and most likely accounting for the high prevalence of these isolates in our enrichments over a wide range of pressures (Fig. 4B and 5) (48, 66, 67). *O. antarctica* RB-8-related ASVs dominated high-pressure enrichments (0.1, 15, and 30 MPa) of hydrocarbon degraders from the Gulf of Mexico following the DWH spill (22)

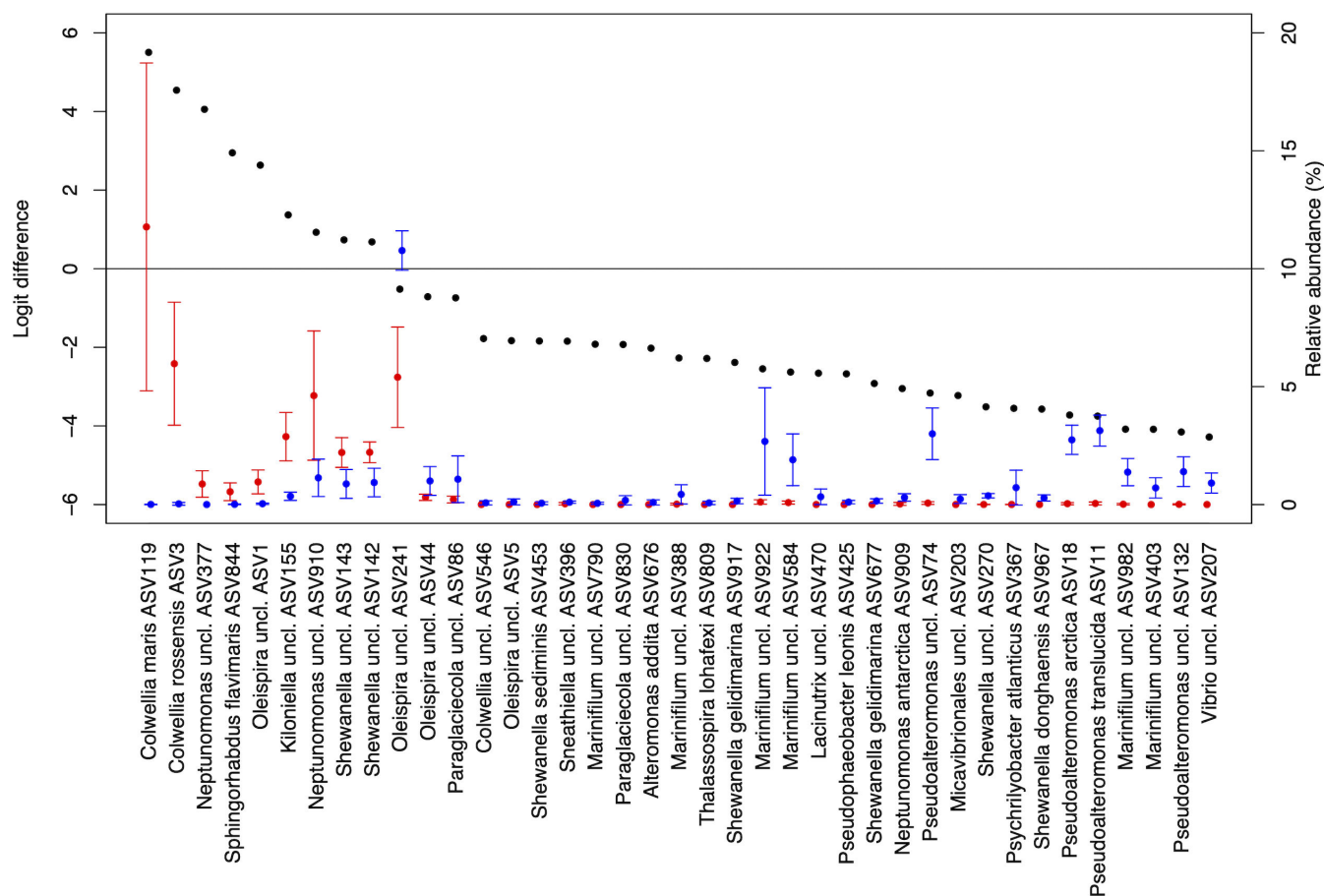


FIG 6 Mean effect size (logit difference, black) and mean relative gene abundance (\pm standard deviation) of ASVs that had significantly higher (logit difference >0) and lower (logit difference <0) relative abundance in the biofilms and medium of the enrichments at 30 MPa (red) after 34 days ($n = 6$) as compared to the lower pressures (0.1–12 MPa, blue) after 20 days ($n = 18$).

of the aforementioned *Colwellia* sp. to produce unsaturated fatty acids could render them more tolerant to increasing pressure.

Piezophilic isolates do not form a monophyletic group, they are spread among the tree of life and are found in psychro-, meso-, and thermophiles, indicating that the required adaptations of life at high pressure are relatively moderate (74). Several of the enriched ASVs at 30 MPa, such as *C. maris* (ASV119), *C. rossensis* (ASV3) and *S. arctica* IR12 (ASV736), were close relatives to psychropiezophilic strains (Fig. 7). Campanaro et al. (75) suggested that the genetic elements conferring pressure adaptation in the deep sea could be laterally transferred. Comparative genomics of pressure-sensitive and piezophilic strains of *Colwellia* sp. found that several piezophile-specific genes were near genomic islands highlighting that adaptation to high pressure may be facilitated by horizontal gene transfer (54). Previously, Marietou and Bartlett (62) have demonstrated that it is possible to isolate culturable high-pressure-surviving bacteria from shallow-water bacterioplankton (South California, USA) that are phylogenetically similar to isolates from deep-sea environments. Moreover, Grossart and Gust (76) observed a pressure-induced shift toward a gammaproteobacterial-dominated community, when they tested the effects of increasing pressure to a simulated sinking (1,000 m/d) shallow water microcosm from surface waters to a 4,000 m depth. Tamburini et al. (77) also reported an increase in the relative abundance of gammaproteobacteria in the microbial community associated with sinking (200 m/d) fecal pellets to 1,500 m depth (15 MPa).

Conclusion

The present study examines the effect of hydrostatic pressure (0.1–30 MPa) on a hydrocarbon-degrading biofilm originally adapted to about 6 MPa. Cell-specific CO₂ production rates provided a clear synthesis of the observed microbial activity: an initial biofilm-dominated bloom (91–93%) of oil degraders with high microbial activities of 0.82–0.90 fmol CO₂-bacterial gene⁻¹·day⁻¹ at 0.1–8 MPa, but undetectable activity at 30 MPa after 6 days. At 30 MPa, the microbial activity increased between days 6 and 34 with an average rate of 0.36 ± 0.08 fmol CO₂-bacterial gene⁻¹·day⁻¹. Bacterial gene sequencing revealed no differences in the microbial community composition at 0–12 MPa. While the typical Arctic alkane degraders *Oleispira* sp. and *Shewanella* sp. were abundant across the different pressures and over time, *Colwellia* sp., *Neptunomonas* sp., and *Kiloniella* sp. were significantly enriched at 30 MPa. Our results suggest that the physiological adaptations of psychrophilic bacteria to thrive at sub-zero temperature make Arctic oil degraders tolerant to mild hydrostatic pressure up to 12 MPa as compared to temperate climate communities showing pressure-induced inhibition at 10–15 MPa in comparable studies. Therefore, the activity of hydrocarbon degraders in sinking marine oil snow in the Arctic may maintain activity down to depths of about 1,200 m, after which pressure can substantially affect hydrocarbon degradation at increasing depth down to 3,000 m.

ACKNOWLEDGMENTS

Lykke Poulsen, Britta Poulsen, and Susanne Nielsen from the Department of Biology, Aarhus University are gratefully acknowledged for their excellent technical laboratory assistance.

This work is a contribution to the Arctic Science Partnership (asp-net.org) and was supported by the research grant 17454 from Villum Fonden and the Multi-Partner Oil Spill Research Initiative (MPRI) of Fisheries and Oceans Canada.

AUTHOR AFFILIATIONS

¹Department of Biology, Section for Microbiology, Aarhus University, Aarhus, Denmark

²Department of Biological and Chemical Engineering, Aarhus University, Aarhus, Denmark

³Arctic Research Centre, Department of Biology, Aarhus University, Aarhus, Denmark

⁴Centre for Water Technology (WATEC), Aarhus University, Aarhus, Denmark

AUTHOR ORCID*s*

Leendert Vergeynst  <http://orcid.org/0000-0002-4388-4315>

FUNDING

Funder	Grant(s)	Author(s)
Villum Fonden (Villum Foundation)	17454	Leendert Vergeynst
Gouvernement du Canada Fisheries and Oceans Canada (DFO)		Søren Rysgaard Leendert Vergeynst

AUTHOR CONTRIBUTIONS

Angeliki Marietou, Conceptualization, Formal analysis, Investigation, Methodology, Supervision, Visualization, Writing – original draft, Writing – review and editing | Jennie Spicker Schmidt, Data curation, Formal analysis, Investigation | Martin R. Rasmussen, Data curation, Formal analysis, Investigation | Alberto Scoma, Conceptualization, Resources, Writing – original draft, Writing – review and editing | Søren Rysgaard, Funding acquisition, Resources, Writing – review and editing | Leendert Vergeynst, Conceptualization, Data curation, Formal analysis, Funding acquisition, Investigation, Methodology, Project administration, Resources, Supervision, Visualization, Writing – original draft, Writing – review and editing

ADDITIONAL FILES

The following material is available [online](#).

Supplemental Material

Table S1 and Fig. S1 to S3 (AEM00987-23-s0001.pdf). Supplemental figures and tables.

REFERENCES

- Barnhart KR, Miller CR, Overeem I, Kay JE. 2016. Mapping the future expansion of Arctic open water. *Nat Clim Change* 6:280–285. <https://doi.org/10.1038/nclimate2848>
- Smith LC, Stephenson SR. 2013. New Trans-Arctic shipping routes navigable by midcentury. *Proc Natl Acad Sci U S A* 110:E1191–E1195. <https://doi.org/10.1073/pnas.1214212110>
- Gautier DL, Bird KJ, Charpentier RR, Grantz A, Houseknecht DW, Klett TR, Moore TE, Pitman JK, Schenk CJ, Schuenemeyer JH, Sørensen K, Tennyson ME, Valin ZC, Wandrey CJ. 2009. Assessment of undiscovered oil and gas in the Arctic. *Science* 324:1175–1179. <https://doi.org/10.1126/science.1169467>
- Brooijmans RJW, Pastink MI, Siezen RJ. 2009. Hydrocarbon-degrading bacteria: the oil-spill clean-up crew. *Microb Biotechnol* 2:587–594. <https://doi.org/10.1111/j.1751-7915.2009.00151.x>
- Wolfe DA, Hameedi MJ, Galt JA, Watabayashi G, Short J, O'Claire C, Rice S, Michel J, Payne JR, Braddock J, Hanna S, Sale D. 1994. The fate of the oil spilled from the Exxon Valdez. *Environ Sci Technol* 28:560A–568A. <https://doi.org/10.1021/es00062a712>
- Atlas RM, Hazen TC. 2011. Oil biodegradation and bioremediation: a tale of the two worst spills in U.S. history. *Environ Sci Technol* 45:6709–6715. <https://doi.org/10.1021/es2013227>
- Larkin K, Donaldson K, McDonough N, Rogers A. 2015. Delving deeper: how can we achieve sustainable management of our deep sea through integrated research? EMB Policy Brief 2. European Marine Board.
- Hua Y, Mirnaghi FS, Yang Z, Hollebone BP, Brown CE. 2018. Effect of evaporative weathering and oil-sediment interactions on the fate and behavior of diluted bitumen in marine environments. Part 1. spill-related properties, oil buoyancy, and oil-particulate aggregates characterization. *Chemosphere* 191:1038–1047. <https://doi.org/10.1016/j.chemosphere.2017.10.156>
- Vergeynst L, Wegeberg S, Aamand J, Lassen P, Gosewinkel U, Fritt-Rasmussen J, Gustavson K, Mosbech A. 2018. Biodegradation of marine oil spills in the Arctic with a Greenland perspective. *Sci Total Environ* 626:1243–1258. <https://doi.org/10.1016/j.scitotenv.2018.01.173>
- Guyomarch J, Le Floch S, Merlin F-X. 2002. Effect of suspended mineral load, water salinity and oil type on the size of oil–mineral aggregates in the presence of chemical dispersant. *Spill Sci Technol Bull* 8:95–100. [https://doi.org/10.1016/S1353-2561\(02\)00118-4](https://doi.org/10.1016/S1353-2561(02)00118-4)
- Passow U, Ziervogel K, Asper V, Diercks A. 2012. Marine snow formation in the aftermath of the *Deepwater Horizon* oil spill in the Gulf of Mexico. *Environ Res Lett* 7:035301. <https://doi.org/10.1088/1748-9326/7/3/035301>
- Rahsepar S, Langenhoff AAM, Smit MPJ, van Eenennaam JS, Murk AJ, Rijnaarts HHM. 2017. Oil biodegradation: interactions of artificial marine snow, clay particles, oil and corexit. *Mar Pollut Bull* 125:186–191. <https://doi.org/10.1016/j.marpolbul.2017.08.021>
- Passow U. 2016. Formation of rapidly-sinking, oil-associated marine snow. *Deep Sea Res Part II Top Stud Oceanogr* 129:232–240. <https://doi.org/10.1016/j.dsr2.2014.10.001>
- Ziervogel K, Joye SB, Arnosti C. 2016. Microbial enzymatic activity and secondary production in sediments affected by the sedimentation pulse following the *Deepwater Horizon* oil spill. *Deep Sea Res Part II Top Stud Oceanogr* 129:241–248. <https://doi.org/10.1016/j.dsr2.2014.04.003>
- Romero IC, Schwing PT, Brooks GR, Larson RA, Hastings DW, Ellis G, Goddard EA, Hollander DJ. 2015. Hydrocarbons in deep-sea sediments following the 2010 *Deepwater Horizon* blowout in the northeast Gulf of

- Mexico. PLoS One 10:e0128371. <https://doi.org/10.1371/journal.pone.0128371>
16. Oil Budget Calculator Science and Engineering Team (U.S.). 2010. Oil budget calculator *Deepwater Horizon*. Federal Interagency Solutions Group, Oil Budget Calculator Science and Engineering Team
 17. Burd AB, Chanton JP, Daly KL, Gilbert S, Passow U, Quigg A. 2020. The science behind marine-oil snow and MOSSFA: past, present, and future. *Prog Oceanogr* 187:102398. <https://doi.org/10.1016/j.pocean.2020.102398>
 18. Hackbusch S, Noirungsee N, Viamonte J, Sun X, Bubenheim P, Kostka JE, Müller R, Liese A. 2020. Influence of pressure and dispersant on oil biodegradation by a newly isolated *Rhodococcus* strain from deep-sea sediments of the Gulf of Mexico. *Mar Pollut Bull* 150:110683. <https://doi.org/10.1016/j.marpolbul.2019.110683>
 19. Nguyen UT, Lincoln SA, Valladares Juárez AG, Schedler M, Macalady JL, Müller R, Freeman KH. 2018. The influence of pressure on crude oil biodegradation in shallow and deep Gulf of Mexico sediments. PLoS One 13:e0199784. <https://doi.org/10.1371/journal.pone.0199784>
 20. Scoma A, Barbato M, Hernandez-Sanabria E, Mapelli F, Daffonchio D, Borin S, Boon N. 2016. Microbial oil-degradation under mild hydrostatic pressure (10 MPa): which pathways are impacted in piezosensitive hydrocarbonoclastic bacteria? *Sci Rep* 6:23526. <https://doi.org/10.1038/srep23526>
 21. Scoma A, Heyer R, Rifai R, Dandyk C, Marshall I, Kerckhof F-M, Marietou A, Boshker HTS, Meysman FJR, Malmos KG, Vosegaard T, Vermeir P, Banat IM, Benndorf D, Boon N. 2019. Reduced TCA cycle rates at high hydrostatic pressure hinder hydrocarbon degradation and obligate oil degraders in natural, deep-sea microbial communities. *ISME J* 13:1004–1018. <https://doi.org/10.1038/s41396-018-0324-5>
 22. Marietou A, Chastain R, Beulig F, Scoma A, Hazen TC, Bartlett DH. 2018. The effect of hydrostatic pressure on enrichments of hydrocarbon degrading microbes from the Gulf of Mexico following the *Deepwater Horizon* oil spill. *Front Microbiol* 9:1050. <https://doi.org/10.3389/fmicb.2018.01050>
 23. Schedler M, Hiessl R, Valladares Juárez AG, Gust G, Müller R. 2014. Effect of high pressure on hydrocarbon-degrading bacteria. *AMB Express* 4:77. <https://doi.org/10.1186/s13568-014-0077-0>
 24. Prince RC, Nash GW, Hill SJ. 2016. The biodegradation of crude oil in the deep ocean. *Mar Pollut Bull* 111:354–357. <https://doi.org/10.1016/j.marpolbul.2016.06.087>
 25. Kampouris ID, Gründger GF, Christensen JH, Greer CW, Kjeldsen KU, Boone W, Meire L, Rysgaard S, Vergeynst L. 2023. Long-term patterns of hydrocarbon biodegradation and bacterial community composition in epipelagic and mesopelagic zones of an Arctic fjord. *J Hazard Mater* 446:130656. <https://doi.org/10.1016/j.jhazmat.2022.130656>
 26. Mortensen J, Lennert K, Bendtsen J, Rysgaard S. 2011. Heat sources for glacial melt in a sub-Arctic fjord (Godthåbsfjord) in contact with the Greenland ice sheet. *J Geophys Res* 116. <https://doi.org/10.1029/2010JC006528>
 27. Nielsen LP, Christensen PB, Revsbech NP, Sørensen J. 1990. Denitrification and oxygen respiration in biofilms studied with a microsensor for nitrous oxide and oxygen. *Microb Ecol* 19:63–72. <https://doi.org/10.1007/BF02015054>
 28. Vergeynst L, Kjeldsen KU, Lassen P, Rysgaard S. 2018. Bacterial community succession and degradation patterns of hydrocarbons in seawater at low temperature. *J Hazard Mater* 353:127–134. <https://doi.org/10.1016/j.jhazmat.2018.03.051>
 29. Lever MA, Torti A, Eickenbusch P, Michaud AB, Šantl-Temkiv T, Jørgensen BB. 2015. A modular method for the extraction of DNA and RNA, and the separation of DNA pools from diverse environmental sample types. *Front Microbiol* 6:476. <https://doi.org/10.3389/fmicb.2015.00476>
 30. Starnawski P, Bataillon T, Etema TJG, Jochum LM, Schreiber L, Chen X, Lever MA, Polz MF, Jørgensen BB, Schramm A, Kjeldsen KU. 2017. Microbial community assembly and evolution in subseafloor sediment. *Proc Natl Acad Sci U S A* 114:2940–2945. <https://doi.org/10.1073/pnas.1614190114>
 31. Ohkuma M, Kudo T. 1998. Phylogenetic analysis of the symbiotic intestinal microflora of the termite *Cryptotermes domesticus*. *FEMS Microbiol Lett* 164:389–395. <https://doi.org/10.1111/j.1574-6968.1998.tb13114.x>
 32. Vergeynst L, Christensen JH, Kjeldsen KU, Meire L, Boone W, Malmquist LMV, Rysgaard S. 2019. *In situ* biodegradation, photooxidation and dissolution of petroleum compounds in Arctic seawater and sea ice. *Water Res* 148:459–468. <https://doi.org/10.1016/j.watres.2018.10.066>
 33. Callahan BJ, McMurdie PJ, Rosen MJ, Han AW, Johnson AJA, Holmes SP. 2016. DADA2: high-resolution sample inference from Illumina amplicon data. *Nat Methods* 13:581–583. <https://doi.org/10.1038/nmeth.3869>
 34. Vergeynst L, Greer CW, Mosbech A, Gustavson K, Meire L, Poulsen KG, Christensen JH. 2019. Biodegradation, photo-oxidation, and dissolution of petroleum compounds in an Arctic Fjord during summer. *Environ Sci Technol* 53:12197–12206. <https://doi.org/10.1021/acs.est.9b03336>
 35. Fernandes AD, Reid JN, MacKlaim JM, McMurrugh TA, Edgell DR, Gloor GB. 2014. Unifying the analysis of high-throughput sequencing datasets: characterizing RNA-seq, 16S rRNA gene sequencing and selective growth experiments by compositional data analysis. *Microbiome* 2:15. <https://doi.org/10.1186/2049-2618-2-15>
 36. Oksanen J, Blanchet FG, Friendly M, Kindt R, Legendre P, McGlenn D, Minchin PR, O'Hara RB, Gavin LS, Solymos P, Henry M, Stevens H, Szoeacs E, Wagner H. 2017. *vegan*: community ecology package.
 37. Aitchison J. 1982. The statistical analysis of compositional data. *J R Stat Soc Series B Stat Methodol* 44:139–160. <https://doi.org/10.1111/j.2517-6161.1982.tb01195.x>
 38. Martín-Fernández JA, Hron K, Templ M, Filzmoser P, Palarea-Albaladejo J. 2015. Bayesian-multiplicative treatment of count zeros in compositional data sets. *Stat Modelling* 15:134–158. <https://doi.org/10.1177/1471082X14535524>
 39. Legendre P, Borcard D, Roberts DW. 2012. Variation partitioning involving orthogonal spatial eigenfunction submodels. *Ecology* 93:1234–1240. <https://doi.org/10.1890/11-2028.1>
 40. Altschul SF, Gish W, Miller W, Myers EW, Lipman DJ. 1990. Basic local alignment search tool. *J Mol Biol* 215:403–410. [https://doi.org/10.1016/S0022-2836\(05\)80360-2](https://doi.org/10.1016/S0022-2836(05)80360-2)
 41. Stamatakis A. 2014. RAxML version 8: a tool for phylogenetic analysis and post-analysis of large phylogenies. *Bioinformatics* 30:1312–1313. <https://doi.org/10.1093/bioinformatics/btu033>
 42. Letunic I, Bork P. 2007. Interactive Tree Of Life (iTOL): an online tool for phylogenetic tree display and annotation. *Bioinformatics* 23:127–128. <https://doi.org/10.1093/bioinformatics/btl529>
 43. Winnes H, Moldanová J, Anderson M, Fridell E. 2016. On-board measurements of particle emissions from marine engines using fuels with different sulphur content. *Proc Inst Mech Eng* 230:45–54. <https://doi.org/10.1177/1475090214530877>
 44. Korczewski Z. 2021. Methodology for determining the elemental composition, as well as energy and ignition properties of the low-sulfur marine fuels. *C Engines* 186:96–102. <https://doi.org/10.19206/CE-141573>
 45. Fukuda R, Ogawa H, Nagata T, Koike I. 1998. Direct determination of carbon and nitrogen contents of natural bacterial assemblages in marine environments. *Appl Environ Microbiol* 64:3352–3358. <https://doi.org/10.1128/AEM.64.9.3352-3358.1998>
 46. Vrede K, Heldal M, Norland S, Bratbak G. 2002. Elemental composition (C, N, P) and cell volume of exponentially growing and nutrient-limited bacterioplankton. *Appl Environ Microbiol* 68:2965–2971. <https://doi.org/10.1128/AEM.68.6.2965-2971.2002>
 47. Braun S, Morono Y, Littmann S, Kuypers M, Aslan H, Dong M, Jørgensen BB, Lomstein Ba. 2016. Size and carbon content of sub-seafloor microbial cells at landsort deep, Baltic sea. *Front Microbiol* 7:1375. <https://doi.org/10.3389/fmicb.2016.01375>
 48. Yakimov MM, Giuliano L, Gentile G, Crisafi E, Chernikova TN, Abraham W-R, Lünsdorf H, Timmis KN, Golyshin PN. 2003. *Oleispira antarctica* gen. nov., sp. nov., a novel hydrocarbonoclastic marine bacterium isolated from Antarctic coastal sea water. *Int J Syst Evol Microbiol* 53:779–785. <https://doi.org/10.1099/ijs.0.02366-0>
 49. Gerdes B, Brinkmeyer R, Dieckmann G, Helmke E. 2005. Influence of crude oil on changes of bacterial communities in Arctic sea-ice. *FEMS Microbiol Ecol* 53:129–139. <https://doi.org/10.1016/j.femsec.2004.11.010>
 50. Jensen S, Lynch MDJ, Ray JL, Neufeld JD, Hovland M. 2015. Norwegian deep-water coral reefs: cultivation and molecular analysis of planktonic microbial communities. *Environ Microbiol* 17:3597–3609. <https://doi.org/10.1111/1462-2920.12531>
 51. Savoca S, Lo Giudice A, Papale M, Mangano S, Caruso C, Spanò N, Michaud L, Rizzo C. 2019. Antarctic sponges from the Terra Nova Bay

- (Ross Sea) host a diversified bacterial community. *Sci Rep* 9:16135. <https://doi.org/10.1038/s41598-019-52491-0>
54. Prasad S, Manasa P, Buddhi S, Tirunagari P, Begum Z, Rajan S, Shivaji S. 2014. Diversity and bioprospective potential (cold-active enzymes) of cultivable marine bacteria from the subarctic glacial Fjord, Kongsfjorden. *Curr Microbiol* 68:233–238. <https://doi.org/10.1007/s00284-013-0467-6>
55. Gontikaki E, Potts LD, Anderson JA, Witte U. 2018. Hydrocarbon-degrading bacteria in deep-water subarctic sediments (Faroe-Shetland Channel). *J Appl Microbiol* 125:1040–1053. <https://doi.org/10.1111/jam.14030>
54. Peoples LM, Kyaw TS, Ugalde JA, Mullane KK, Chastain RA, Yayanos AA, Kusube M, Methé BA, Bartlett DH. 2020. Distinctive gene and protein characteristics of extremely piezophilic *Colwellia*. *BMC Genomics* 21:692. <https://doi.org/10.1186/s12864-020-07102-y>
55. Gomes A, Christensen JH, Gründger F, Kjeldsen KU, Rysgaard S, Vergeynst L. 2022. Biodegradation of water-accommodated aromatic oil compounds in Arctic seawater at 0 °C. *Chemosphere* 286:131751. <https://doi.org/10.1016/j.chemosphere.2021.131751>
56. Head IM, Jones DM, Röling WFM. 2006. Marine microorganisms make a meal of oil. *Nat Rev Microbiol* 4:173–182. <https://doi.org/10.1038/nrmicro1348>
57. Kaur J, Vishnu AL, Khipla N, Kaur J. 2022. Microbial life in cold regions of the deep sea, p 63–86. In Goel R, R Soni, DC Suyal, M Khan (ed), *Survival strategies in cold-adapted microorganisms*. Springer, Singapore. <https://doi.org/10.1007/978-981-16-2625-8>
58. Bartlett DH. 2002. Pressure effects on *in vivo* microbial processes. *Biochim Biophys Acta* 1595:367–381. [https://doi.org/10.1016/s0167-4838\(01\)00357-0](https://doi.org/10.1016/s0167-4838(01)00357-0)
59. Grossi V, Yakimov MM, Al Ali B, Tapilatu Y, Cuny P, Goutx M, La Cono V, Giuliano L, Tamburini C. 2010. Hydrostatic pressure affects membrane and storage lipid compositions of the piezotolerant hydrocarbon-degrading *Marinobacter hydrocarbonoclasticus* strain #5. *Environ Microbiol* 12:2020–2033. <https://doi.org/10.1111/j.1462-2920.2010.02213.x>
60. Allen EE, Facciotti D, Bartlett DH. 1999. Monounsaturated but not polyunsaturated fatty acids are required for growth of the deep-sea bacterium photobacterium profundum SS9 at high pressure and low temperature. *Appl Environ Microbiol* 65:1710–1720. <https://doi.org/10.1128/AEM.65.4.1710-1720.1999>
61. Marietou A, Nguyen ATT, Allen EE, Bartlett DH. 2014. Adaptive laboratory evolution of *Escherichia coli* K-12 MG1655 for growth at high hydrostatic pressure. *Front Microbiol* 5:749. <https://doi.org/10.3389/fmicb.2014.00749>
62. Marietou A, Bartlett DH. 2014. Effects of high hydrostatic pressure on coastal bacterial community abundance and diversity. *Appl Environ Microbiol* 80:5992–6003. <https://doi.org/10.1128/AEM.02109-14>
63. Lauro FM, Chastain RA, Blankenship LE, Yayanos AA, Bartlett DH. 2007. The unique 16S rRNA genes of piezophiles reflect both phylogeny and adaptation. *Appl Environ Microbiol* 73:838–845. <https://doi.org/10.1128/AEM.01726-06>
64. Scoma A. 2021. Functional groups in microbial ecology: updated definitions of piezophiles as suggested by hydrostatic pressure dependence on temperature. *ISME J* 15:1871–1878. <https://doi.org/10.1038/s41396-021-00930-0>
65. Hazen TC, Dubinsky EA, DeSantis TZ, Andersen GL, Piceno YM, Singh N, Jansson JK, Probst A, Borglin SE, Fortney JL, et al. 2010. Deep-sea oil plume enriches indigenous oil-degrading bacteria. *Science* 330:204–208. <https://doi.org/10.1126/science.1195979>
66. Kube M, Chernikova TN, Al-Ramahi Y, Belouqui A, Lopez-Cortez N, Guazzaroni M-E, Heipieper HJ, Klages S, Kotsyurbenko OR, Langerl, et al. 2013. Genome sequence and functional genomic analysis of the oil-degrading bacterium *Oleispira antarctica*. *Nat Commun* 4:2156. <https://doi.org/10.1038/ncomms3156>
67. Wang Y, Yu M, Austin B, Zhang X-H. 2012. *Oleispira lenta* sp. nov., a novel marine bacterium isolated from Yellow sea coastal seawater in Qingdao, China. *Antonie Van Leeuwenhoek* 101:787–794. <https://doi.org/10.1007/s10482-011-9693-8>
68. Yang T, Nigro LM, Gutierrez T, D'Ambrosio L, Joye SB, Highsmith R, Teske A. 2016. Pulsed blooms and persistent oil-degrading bacterial populations in the water column during and after the *Deepwater Horizon* blowout. *Deep Sea Res Part II Top Stud Oceanogr* 129:282–291. <https://doi.org/10.1016/j.dsr2.2014.01.014>
69. Brakstad OG, Nonstad I, Faksness L-G, Brandvik PJ. 2008. Responses of microbial communities in Arctic sea ice after contamination by crude petroleum oil. *Microb Ecol* 55:540–552. <https://doi.org/10.1007/s00248-007-9299-x>
70. Powell SM, Bowman JP, Snape I. 2004. Degradation of nonane by bacteria from Antarctic marine sediment. *Polar Biol* 27:573–578. <https://doi.org/10.1007/s00300-004-0639-8>
71. Redmond MC, Valentine DL. 2012. Natural gas and temperature structured a microbial community response to the *Deepwater Horizon* oil spill. *Proc Natl Acad Sci U S A* 109:20292–20297. <https://doi.org/10.1073/pnas.1108756108>
72. Bowman JP, Gosink JJ, McCammon SA, Lewis TE, Nichols DS, Nichols PD, Skerratt JH, Staley JT, McMeekin TA. 1998. *Colwellia demingiae* sp. nov., *Colwellia hornerae* sp. nov., *Colwellia rossensis* sp. nov. and *Colwellia psychrotropica* sp. nov.: psychrophilic Antarctic species with the ability to synthesize docosahexaenoic acid (22:6ω3). *Int J Syst Bacteriol* 48:1171–1180. <https://doi.org/10.1099/00207713-48-4-1171>
73. Yumoto I, Kawasaki K, Iwata H, Matsuyama H, Okuyama H. 1998. Assignment of *Vibrio* sp. strain ABE-1 to *Colwellia maris* sp. nov., a new psychrophilic bacterium. *Int J Syst Bacteriol* 48 Pt 4:1357–1362. <https://doi.org/10.1099/00207713-48-4-1357>
74. Bartlett DH, Lauro FM, Eloë EA. 2007. Microbial adaptation to high pressure, p 331–348. In *Physiology and biochemistry of extremophiles*. John Wiley & Sons, Ltd. <https://doi.org/10.1128/9781555815813>
75. Campanaro S, Zezzi A, Vitulo N, Lauro FM, D'Angelo M, Simonato F, Cestaro A, Malacrida G, Bertoloni G, Valle G, Bartlett DH. 2005. Laterally transferred elements and high pressure adaptation in *Photobacterium profundum* strains. *BMC Genomics* 6:122. <https://doi.org/10.1186/1471-2164-6-122>
76. Grossart HP, Gust G. 2009. Hydrostatic pressure affects physiology and community structure of marine bacteria during settling to 4000 m: an experimental approach. *Mar Ecol Prog Ser* 390:97–104. <https://doi.org/10.3354/meps08201>
77. Tamburini C, Goutx M, Guigue C, Garel M, Lefèvre D, Charrière B, Sempéré R, Pepa S, Peterson ML, Wakeham S, Lee C. 2009. Effects of hydrostatic pressure on microbial alteration of sinking fecal pellets. *Deep Sea Res Part II Top Stud Oceanogr* 56:1533–1546. <https://doi.org/10.1016/j.dsr2.2008.12.035>